processes

MDPI

Review

Fe_3O_4 Core–Shell Nanostructures with Anticancer and Antibacterial Properties: A Mini-Review

Miruna-Adriana Ioța [1,2], Laura-Mădălina Cursaru [1,*], Adriana-Gabriela Șchiopu [3], Ioan Albert Tudor [1], Adrian-Mihail Motoc [1,*] and Roxana Mioara Piticescu [1]

[1] National Research-Development Institute for Non-Ferrous and Rare Metals—IMNR, 102 Biruintei Blvd., 077145 Pantelimon, Romania; iota.miruna@imnr.ro (M.-A.I.); atudor@imnr.ro (I.A.T.); roxana.piticescu@imnr.ro (R.M.P.)
[2] Interdisciplinary Doctoral School, University of Pitești, 110040 Pitești, Romania
[3] Department of Manufacturing and Industrial Management, University of Pitești, 110040 Pitești, Romania; gabriela.plaiasu@upit.ro
* Correspondence: mpopescu@imnr.ro (L.-M.C.); amotoc@imnr.ro (A.-M.M.); Tel.: +40-21-352-20-46 (L.-M.C. & A.-M.M.)

Abstract: Core–shell nanoparticles are functional materials with tailored properties, able to improve the requirements of various applications. Both core and shell components can be inorganic or organic, and there are numerous studies in this field regarding their synthesis methods, properties, and applications. This review aims to study core–shell nanostructures with Fe_3O_4 cores and different shell types, observing their antibacterial and anticancer properties. By the type of coating, Fe_3O_4 core–shell nanoparticles (NPs) are classified into four categories: metal-coated NPs, metal-organic framework (MOF) coated NPs, metal oxide coated NPs, and polymer-coated NPs. Each category is briefly presented, emphasizing anticancer or antibacterial properties and specific applications (cancer diagnosis or therapy, drug carrier). Moreover, synthesis methods and particle size for both core and shell nanostructures, as well as the magnetic properties of the final core–shell material, are summarized in this review. Most of the consulted papers discussed sphere-like core–shell nanoparticles obtained by chemical methods such as coprecipitation, hydrothermal, and green synthesis methods using plant extract. These types of core–shell nanoparticles could be used as drug nanocarriers for tumor-targeted drug delivery, hyperthermia treatment, or contrast agents. Further work needs to be conducted to understand nanoparticles' interaction with living cells and their traceability in the human body.

Keywords: iron oxide; core–shell nanostructures; magnetic properties; anticancer properties; antibacterial properties; cancer therapy

Citation: Ioța, M.-A.; Cursaru, L.-M.; Șchiopu, A.-G.; Tudor, I.A.; Motoc, A.-M.; Piticescu, R.M. Fe_3O_4 Core–Shell Nanostructures with Anticancer and Antibacterial Properties: A Mini-Review. *Processes* **2023**, *11*, 1882. https://doi.org/10.3390/pr11071882

Received: 30 May 2023
Revised: 18 June 2023
Accepted: 21 June 2023
Published: 23 June 2023

1. Introduction

Fe_3O_4 nanoparticles, due to their physical–chemical properties, low toxicity, and high saturation magnetization values, have received great attention in the biomedical field. Their pharmaceutical applications, such as anticancer agents against various cancer cells and antiviral (e.g., influenza virus, HBV, HIV) or antibacterial agents, have been recently considered. They are studied in several areas of interest from a medical point of view, such as magnetic hyperthermia, drug delivery, magnetic resonance imaging, photothermal therapy of tumors, magnetic bioseparation, magnetofection agents, DNA molecule detection, infectious diseases, and cancer therapy [1–30].

In chemotherapy, several drug delivery systems can be used, but among them, one has shown great potential in nanomedicine: superparamagnetic iron oxide nanoparticles, also known as SPION, have become a priority choice for the delivery of cancer drugs because they effectively target cancer cells, through a magnetic field, improving the accumulation of magnetic nanoparticles at the target site. Moreover, these nanoparticles (NPs) also make simultaneous

drug delivery and magnetic resonance imaging possible [31,32]. SPIONs have been extensively studied for cancer treatment by magnetic hyperthermia. The principle of this technique is as follows: when iron oxide NPs are exposed to an external magnetic field, magnetic losses are dissipated as heat appears. If SPIONs are placed near tumors, they raise the temperature of the tumor to a therapeutic level (42–45 °C) and induce weakness or death of cancer cells without damaging the surrounding healthy tissue or cells [1,18,33–35]. Several studies have provided evidence that the overuse of antibiotics has led to the development of bacterial resistance to numerous drugs, as in the case of nosocomial infections in hospitals [36,37]. Recently, researchers found that iron oxide nanoparticles could be used as magnetic drug delivery systems for antibiotics (e.g., amoxicillin). It means that Fe_3O_4 is loaded with various antibiotics as agents for killing bacteria in the respective damaged tissue, reducing the dose of medication needed in the classical method. When the external magnetic field is applied, the affected tissue is heated, and antibiotics act as bacteria-killing heat agents. A new approach is represented by the green synthesis method of Fe_3O_4 in the presence of plant extracts [36]. For example, Fe_3O_4 prepared using garlic extract has potential antibacterial action and is tested in the antimicrobial therapy of numerous multidrug-resistant bacterial strains and fungi. However, bare SPION oxidizes easily in the air, losing its magnetic properties and dispersibility due to its high chemical activity [38]. Therefore, surface coating is recommended to maintain the stability of magnetic Fe_3O_4 and to improve iron oxide antimicrobial applications. Moreover, the surface coating prevents agglomeration of nanoparticles, protects nanoparticles against reticuloendothelial system (RES) uptake and elimination, and improves internalization efficiency [4,34]. One of the most popular surface coating techniques is the obtaining of core–shell nanostructures. Core–shell particles serve as storage and carrier platforms for many applications [39–41]. Several types of core–shell structures based on Fe_3O_4 (core) have been investigated and have been used in the field of chemotherapy due to both their antibacterial properties and their superparamagnetic properties [32,33,42–46]. This structure is frequently used as a platform for targeted drug delivery in cancer treatment [46]. Bacterial infections and cancer are connected diseases that have become a global health threat. Bacteria accelerate the development of cancer, prompting researchers to find an antibacterial and anticancer drug delivery agent. A lot of articles have studied organic coatings of iron oxide nanoparticles, the most popular being natural and synthetic polymers such as chitosan, dextran, starch, polyethylene glycol (PEG), polyvinyl alcohol (PVA), polyvinyl pyrrolidone (PVP), polyethyleneimine (PEI), poloxamers, polysorbate 20 and 80, thermo-responsive poly (N-isopropyl acrylamide) (PNIPAAm), or small organic molecules with functional groups, such as thiols, amines, or carboxyls [2,4,32,34,47]. In this mini-review, core–shell nanoparticles having Fe_3O_4 as a core will be discussed, describing briefly their properties, synthesis methods, and biomedical applications and focusing on the inorganic shell types. Each synthesis method can produce different sizes, shapes, or magnetic properties for a specific application. The main characteristics of the inorganic core–shell materials discussed in this paper are presented synthetically in the form of tables.

2. Different Types of Core–Shell Structures with Fe_3O_4 Core for Biomedical Applications

Core–shell nanostructures are defined as heterogeneous nanoparticles composed of two or more nanomaterials that can be identified and are separated by distinct boundaries. Both core and shell components can be inorganic (metals, metal oxides) or organic (polymers, biomolecules) [48–50]. Core/shell composite nanostructures (NSs) have attracted much attention in recent years due to their diverse and unique material properties not shown by the core or shell materials alone, such as good mechanical, thermal, and optical properties [48,51]. These properties are significantly enhanced compared to pure compounds [51]. The interaction between the core and the shell of a nanostructure can lead to new properties and functions [45].

There are numerous core–shell materials with various applications and much literature about their classification and detailed descriptions of the preparation method. This paper presents only inorganic core–shell materials with Fe_3O_4 as the core and their medical applications.

Fe_3O_4 can be coated with different types of shells, such as metals (Ag, Au) [52–56], metal–organic frameworks (Cu–MOF), metal oxides (SiO_2, TiO_2, ZnO), and organic polymers (polyethyleneimine: PEI, polyacrylic acid: PAA, etc.), to obtain core–shell nanostructures with desired properties [3].

Core–shell nanostructures with Fe_3O_4 as a core have been a popular research topic over the last decade, with more than 700 articles published in the field, as shown in Figure 1a. As can be seen from Figure 1b, most of the papers published on this topic were research articles (>700 papers) and short communications (>40 papers). The data presented in Figure 1 were obtained using the ScienceDirect database (https://www.sciencedirect.com/) and searching for "Fe_3O_4 core–shell nanoparticles for biomedical applications". The results were refined by year (selecting from 2012 to 2023) in Figure 1a and by article type in Figure 1b. These data were collected in May 2023.

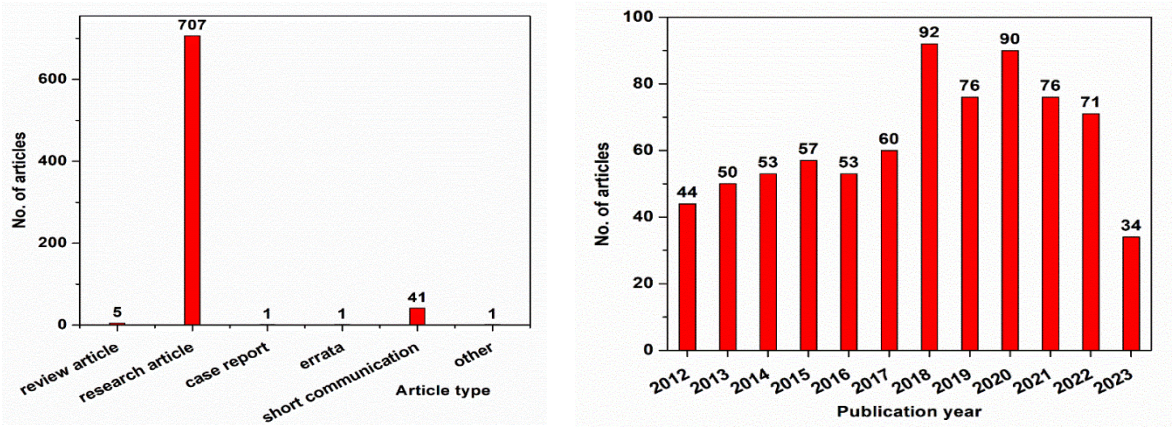

Figure 1. (**a**) Evolution of the published articles in the field of Fe_3O_4 core–shell nanoparticles; (**b**) types of papers published in the field of Fe_3O_4 core–shell nanoparticles.

2.1. Metal-Coated Fe_3O_4

Silver-coated Fe_3O_4 nanohybrids have been used in a broad range of applications, including chemical and biological sensors [48,57], drug delivery—as successful drug carriers with focused antimicrobial, anticancer properties [48,58], diagnosis, and cancer therapy [48,59,60].

Different methods were used to synthesize Ag-coated Fe_3O_4 nanoparticles. Generally, a two-step synthesis procedure is applied: magnetite is prepared by a solvothermal, co-precipitation, or microemulsion route [57,61,62], obtaining spherical-shaped particles, and then Fe_3O_4 nanoparticles are dispersed in $AgNO_3$ solution in the presence of an organic solvent (ethanol, di-chlorobenzene), a surfactant (oleylamine, cetyltrimethylammonium bromide—CTAB), and a reduction agent for Ag (butylamine, sodium borohydride). Another approach uses combined phyto- and hydrothermal synthesis, preparing the magnetite core in the presence of a plant extract (neem leaf extract, leaf extract of *Eryngium planum*, *Vitis vinifera* (grape) stem extract, *Euphorbia peplus* Linn leaf extract), followed by hydrothermal synthesis of Fe_3O_4–Ag (silver nitrate was added in the magnetite suspension). Plant extract acts as a reducing agent for silver shells [44,59,63,64]. Spherical core–shell structures with 7–80 nm are obtained in these cases [44,57,59,61–64]. Moreover, brick-like Ag-coated Fe_3O_4 nanoparticles with ~13 nm in width and ~15 nm in length were prepared by single-step thermal decomposition of the magnetite precursors in the presence of $AgNO_3$ salt and 1,2-hexadecane-diol reduction agent [58].

It has been discovered that Fe_3O_4–Ag nanocomposites present a self-sterilizing property that avoids the formation of biofilms, which are the most dangerous source capable of spreading toxic bacteria into the environment [61], improving the contrast of magnetic resonance imaging (MRI) in cancer detection [48].

Similar synthesis methods as in the case of silver-doped magnetite core–shell structures (coprecipitation, thermal decomposition of Fe_3O_4), followed by reduction of $HAuCl_4$ or gold acetate with various agents ($NaBH_4$, sodium citrate, 1,2-hexadecane-diol), as well as combined phyto-hydrothermal synthesis (with *Juglans regia* green husk as reducing and stabilizing agent for $HAuCl_4$), were reported in [65–72] for gold-coated magnetite nanostructures. In 2023, Danafar et al. [65] prepared Fe_3O_4–Au hybrid nanoparticles coated with bovine serum albumin (BSA) by co-precipitation of magnetite at 60 °C followed by the reduction of $HAuCl_4$ with sodium citrate and $NaBH_4$, resulting in Fe_3O_4–Au hybrids that were further coated with BSA under magnetic stirring at room temperature. They studied their potential application as a contrast agent in magnetic resonance imaging (cancer diagnosis). Gold nanoparticles represent a good option for Fe_3O_4 coating due to their good biocompatibility, large specific surface area, "surface plasmon" property, and well-known attraction for thiol groups from organic molecules [66]. Fe_3O_4–Au core–shell nanoparticles can be used in biomedical applications such as magnetic resonance imaging, hyperthermia, biosensors, immunosensors, photothermal therapy, controlled drug delivery, targeted gene delivery, protein separation, DNA detection, and DNA/RNA interaction [67–71].

2.2. Metal–Organic Framework (MOF) Coated Fe_3O_4

Fe_3O_4 nanoparticle was used as a core for improving the physicochemical properties and the thermal stability of the Cu–MOF compound. Metal–organic frameworks (MOFs) are a class of crystalline, porous materials composed of metal ions surrounded by multi-dented organic molecules. The metal ions form nodes that bind the arms of the organic ligands which act as linkers in the cage-like network structure. MOFs have a high surface area, significant porosity, tunable pore size, and high thermal stability in comparison to other nanostructures. Azizabadi et al. [51] prepared Fe_3O_4–Cu–MOFs by an ultrasonic-assisted reverse micelle synthesis (ultrasonic irradiation time of 10 min, temperature of 25 °C, power of 80 W) and found that this core–shell composite has good antibacterial activities against both Gram-positive and Gram-negative bacteria, which recommends it for advanced biomedical applications.

2.3. Metal Oxide-Coated Fe_3O_4

One of the most studied metal oxides as a shell for the Fe_3O_4 core was SiO_2, due to the powerful attraction of magnetic nanoparticles to silica [73]. SiO_2 particles are non-toxic, highly biocompatible, and abundant in surface hydroxyl groups, which makes them an ideal surface functional coating for magnetic nanoparticles in the medical field [3,74–79]. Fe_3O_4 nanoparticles coated with SiO_2 shells obtained by Ta et al. through hydrolysis and condensation [75] showed increased biocompatible properties and provided new ideas for future bioconjugation studies [3]. Moreover, the Fe_3O_4–SiO_2 core–shell structure prepared by Lu et al. using an ultrasound-assisted method [80] has good opportunities in the field of biomedicine [3].

TiO_2 is another metal oxide with interesting properties such as biocompatibility, chemical inertness, high stability, and resistance to body fluids that lead to its use in cosmetics, pharmaceutics, and malignant tumor therapy [43,81,82]. The coating of magnetite nanoparticles with a TiO_2 shell protects the core from environmental damage and improves biocompatible properties [43]. Fe_3O_4–TiO_2 core–shell structures with various Fe_3O_4:TiO_2 molar ratios were synthesized by a modified sol–gel method [83] or hydrothermal process [84]. The obtained Fe_3O_4–TiO_2 core–shell nanorods are superparamagnetic and could be further used for magnetic hyperthermia applications [43].

Fe_3O_4–ZnO core–shell nanoparticles represent some of the most studied materials for magnetic hyperthermia and bio-imaging applications [33,85–89]. ZnO is well known for its anti-bacterial and biocompatible properties and possesses unique physical and chemical characteristics due to its wide bandgap and elevated exciton binding energy (piezoelectricity, photoluminescence, chemical stability) [90–92]. It has been demonstrated that ZnO–Fe_3O_4 composites combine the magnetic properties of Fe_3O_4 with the antibacte-

rial activity of ZnO, resulting in a material with improved biocompatibility and enhanced antibacterial activity. ZnO–Fe_3O_4 composites inhibit microorganisms' biofilm formation due to their synergetic activity of ion lixiviation (Fe^{3+}, Zn^{2+}) and oxidative activity. The material's magnetic properties play a major role in reducing the ability of microorganisms to attach to different surfaces, inhibiting biofilm formation [85]. It is very important to hinder the formation of biofilm because its existence makes microorganisms more resistant to antibiotics. ZnO/Fe_3O_4 composites have shown enhanced antibacterial ability under visible light irradiation compared to single ZnO [93]. In 2021, Gupta et al. [33] reported the hydrothermal synthesis of Fe_3O_4–ZnO core–shell nanoparticles. The obtained material preserved the photoluminescence capacity of ZnO and the superparamagnetic properties of Fe_3O_4, demonstrating its potential use for hyperthermia therapy and fluorescent-based cellular imaging. Fe_3O_4–ZnO nanoparticles significantly reduced the viability of human cervical cancer cells (HeLa) under the applied AC magnetic field. However, in 2018, Madhubala et al. [87] found that only the lowest concentrations of Fe_3O_4–ZnO core–shell nanoparticles are non-toxic for cells and could be used for cancer treatment using magnetic hyperthermia therapy (MHT). Moreover, the authors concluded that Fe_3O_4–ZnO with a molar ratio of 1:20 has a small particle size and high crystallinity, and Fe_3O_4 is completely encapsulated in the ZnO nanoparticles [87].

2.4. Polymer-Coated Fe_3O_4

Magnetite surface coating with natural or synthetic polymers has been widely investigated [3,32,94–100] due to their good biocompatibility, biodegradability, non-toxicity, stability, and ability to modify physical-chemical surface properties. Covering magnetite with polymers improves the antibacterial and anticancer properties of core–shell nanoparticles. Different polymers such as polyethylene glycol (PEG), chitosan, poly-N-vinylpyrrolidone (PVP), hydroxyl ethylene cellulose (HEC), nanocrystalline cellulose (NCC), heparin-poloxamer (HP), poly(N-isopropyl acrylamide) (PNIPAAm), polyethyleneimine (PEI), and polyacrylic acid (PAA) have been coated on the Fe_3O_4 surface for tumor-targeted drug delivery. In 2021, Mohammadi et al. [95] synthesized magnetic nanoparticles with cross-linked PEG coatings using plasma treatment. The plasma-induced graft polymerization creates a cross-linked network of PEG chains, resulting in a rigid surface that hinders the burst release of the drug. The classical coprecipitation method of magnetite core followed by direct addition of chitosan or PEG shell and heating at 80 °C for 30 min [96] leads to an irregular and dendrimer-like surface morphology with small and large grain sizes. Fe_3O_4 surface functionalized with PEG has significant results at 20 mg/mL against antimicrobial activities. The anticancer activity was tested against HepG2 liver cancer cell lines, and magnetite-polymer nanoparticles are suitable for hyperthermia therapy to treat carcinoma.

When superparamagnetic iron oxide nanoparticles (SPIONs) were coated with heparin-poloxamer (HP) and the core–shell system was tested for anticancer drug delivery, doxorubicin (DOX) was entrapped in the polymer shell, showing a controlled release up to 120 h without any initial burst effect [98]. Moradi et al. [32] prepared Fe_3O_4 core–shell nanoparticles as drug nanocarriers, having PNIPAAm grafted with chitosan as a polymer shell. PNIPAAm is a thermo-responsive polymer, while chitosan is a pH-responsive moiety. Therefore, the highest release percentage of methotrexate (MTX) as a negatively charged anticancer drug has been observed at T = 40 °C and pH = 5.5.

A schematic representation of Fe_3O_4-based core–shell nanoparticles with various types of shells for biomedical applications is shown in Figure 2.

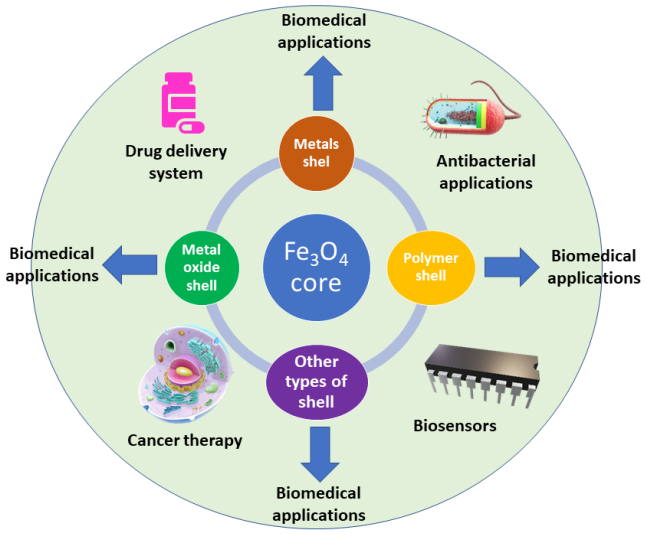

Figure 2. Various types of Fe_3O_4 core–shell nanoparticles with biomedical applications.

Table 1 shows the main synthesis methods and applications of Fe_3O_4 core–shell nanoparticles. Table 2 presents the sizes and properties of core, shell, and core–shell nanoparticles in correlation with the synthesis conditions of the core–shell nanostructure.

Table 1. Synthesis methods for Fe_3O_4 core–shell nanoparticles and their applications.

Type of Core–Shell Material	Core Synthesis Method	Shell Synthesis Method	Application	Reference
Fe_3O_4–Ag Molar ratios: 1:5, 1:10, and 1:20.	Fe_3O_4 nanoparticles were synthesized using neem leaf extract, $FeSO_4$*$7H_2O$, and $Fe(NO_3)_3$*$9H_2O$.	Fe_3O_4–Ag was prepared by hydrothermal method, adding $AgNO_3$ in Fe_3O_4 solution.	Promising anticancer agents.	[44]
Fe_3O_4–Ag	Magnetite was prepared using $FeCl_3$*$6H_2O$, sodium acetate, ethylene glycol, and polyethylene glycol PEG (MW~3000Da).	The silver coating was obtained by adding butylamine to a silver nitrate solution dispersed in ethanol.	Magnetic separation and magnetic resonance imaging (MRI).	[57]
Fe_3O_4–Ag	Fe_3O_4 was prepared by microemulsion technique using ferrous and ferric ammonium sulfate and surfactant CTAB.	Silver-coated magnetite nanoparticles were prepared by microemulsion technique using silver nitrate.	Biomedical applications	[62]
Fe_3O_4–Ag	Fe_3O_4 nanoparticles were prepared using an eco-friendly method. Precursors: *V. vinifera* stem extract, $FeCl_3$*$6H_2O$, and sodium acetate.	$AgNO_3$ was added to the Fe_3O_4 solution, stirring for 2 h. The morphology of the core–shell nanoparticles is nearly spherical with ~32 nm diameter. Particle size is controlled by the addition of *Vitis Vinifera* stem extract which acts as the green solvent, reducing and capping agent.	High antibacterial activity against Gram-negative and Gram-positive pathogens.	[63]
Fe_3O_4–Au	Fe_3O_4 was prepared by coprecipitation method using $FeCl_3$*$6H_2O$ and $FeCl_2$*$4H_2O$.	Fe_3O_4 was mixed with $HAuCl_4$ at 90 °C for 5 min and then sodium citrate was added.	Cancer therapy	[71]
Fe_3O_4–Au	Coprecipitation method using $FeCl_3$*$6H_2O$ and $FeCl_2$*$4H_2O$.	Green synthesis method: Fe_3O_4 nanoparticles were suspended in $HAuCl_4$ solution using *J. regia* (walnut) as a reducing agent.	Cancer treatment	[72]
Fe_3O_4–Cu–MOF	-	Ultrasonic-assisted reverse micelle synthesis using Cu $(NO_3)_2$*$5H_2O$, PVP (polyvinyl pyrrolidone), acetic acid, and Fe_3O_4 nanoparticles.	Good antibacterial activities against both Gram-positive and Gram-negative bacteria.	[51]

Table 1. *Cont.*

Type of Core–Shell Material	Core Synthesis Method	Shell Synthesis Method	Application	Reference
Fe_3O_4–SiO_2	Fe_3O_4 was synthesized by coprecipitation method starting from $FeCl_3$*$6H_2O$ and $FeSO_4$*$4H_2O$.	Fe_3O_4–SiO_2 were obtained by in situ coprecipitation method, adding ethanol, NH_3, and tetraethyl orthosilicate (TEOS) in ethanol.	immune-magnetic separation, separating biomolecules in biomedical and bioprocess engineering.	[73]
Fe_3O_4–SiO_2	Fe_3O_4 was synthesized by coprecipitation method using $FeCl_3$*$6H_2O$ and $FeCl_2$*$4H_2O$.	Fe_3O_4 was dispersed in a mixture of water, ethanol, and NH_3. TEOS was added. Fe_3O_4 nanoparticles were coated with SiO_2 through hydrolysis and condensation.	Bio-applications. Investigation of T cell removal in bone marrow transplantation.	[75]
Fe_3O_4–SiO_2	Fe_3O_4 was prepared by a modified hydrothermal method, starting from $FeCl_3$*$6H_2O$, sodium acetate, and sodium citrate.	Fe_3O_4–SiO_2 nanoparticles were prepared by an ultrasound-assisted method, using TEOS.	Potential use in the field of catalysis, gas separation, and biomedicine.	[80]
Fe_3O_4–SiO_2	Fe_3O_4 was synthesized by coprecipitation method using $FeCl_3$*$6H_2O$ and $FeCl_2$*$4H_2O$ and carboxymethyl cellulose as capping agent.	Fe_3O_4 was dispersed in ethanol and then TEOS was added resulting SiO_2 shell around Fe_3O_4 (modified Stöber process).	Biomedical and solar cell applications.	[78]
Fe_3O_4–TiO_2 Different molar ratios: 1:5, 1:10, and 1:20.	Fe_3O_4 was prepared by phytogenic method using $FeSO_4$, $Fe(NO_3)_3$ and neem leaf extract.	Hydrothermal synthesis of TiO_2 in the presence of Fe_3O_4 to obtain Fe_3O_4–TiO_2 core–shell nanorods.	Potential use for magnetic hyperthermia applications.	[43]
Fe_3O_4–TiO_2	Fe_3O_4 was prepared by coprecipitation method using $FeCl_3$*$6H_2O$ and $FeCl_2$*$4H_2O$.	For TiO_2 coating, $TiCl_4$ was diluted in ethanol and then mixed with Fe_3O_4 solution in ethanol (modified sol–gel synthesis).	Photocatalyst for treating the organic contaminant in the field of environmental protection.	[83]
Fe_3O_4–TiO_2	Solvothermal method using $FeCl_3$ and different surfactants (ethylene glycol, oleic acid, sodium dodecyl sulfate, polyvinylpyrrolidone, polyethylene glycol).	Hydrothermal synthesis using titanium butoxide and ethanol.	drug delivery, hyperthermia treatment, photocatalytic water purification.	[84]
Fe_3O_4–ZnO (molar ratio 1:1)	The hydrothermal approach using ferric (III) acetylacetonate.	Hydrothermal method using zinc acetylacetonate dihydrate.	Potential use in magnetic hyperthermia and bio-imaging.	[33]
Fe_3O_4–ZnO (molar ratio 1:1)	Microwave method using ferric (III) acetylacetonate.	Zinc acetate was added to the Fe_3O_4 suspension which was further subjected to microwave treatment.	Potential for anti-biofilm formulation.	[85]
Fe_3O_4–ZnO	Phyto-synthesis of Fe_3O_4 using $FeSO_4$, $FeNO_3$ and neem extract.	Hydrothermal synthesis of Fe_3O_4–ZnO using $ZnCl_2$.	Useful for Magnetic Hyperthermia Therapy (MHT) for cancer treatment.	[87]
Fe_3O_4–chitosan–Ag	Suspension technique for Fe_3O_4–chitosan synthesis using commercial magnetite and chitosan powders.	Fe_3O_4–chitosan was dispersed in DMF (dimethylformamide) and mixed with $AgNO_3$ and glucose.	potential antimicrobial agents or additives in medical, biological, food packaging, and textile applications.	[100]
Fe_3O_4–heparine–poloxamer (HP)	Fe_3O_4 was prepared by coprecipitation method using $FeCl_3$*$6H_2O$ and $FeCl_2$*$4H_2O$.	Fe_3O_4–HP core–shell system was prepared by ultrasonication.	Drug delivery system for cancer treatment.	[98]
Fe_3O_4–PNIPAAm	Coprecipitation in Ar atmosphere, using $FeCl_2$ and $FeCl_3$.	Polymerization of NIPAAm in the presence of Fe_3O_4 at 90 °C for 5 days.	Targeted drug delivery against human lung and breast cancer.	[32]

Table 2. Size and properties of Fe_3O_4-based core–shell nanostructures.

Type of Core–Shell Material	Synthesis Conditions	Core Diameter	Shell Thickness	Properties	Reference
Fe_3O_4–Ag	Hydro-thermal synthesis at 200 °C/18 h.	45 nm	5 nm.	Super-paramagnetic behavior at 300 K. magnetization: 12.64 emu/g. Cytotoxic behavior on liver cancer cells.	[44]
Fe_3O_4–Ag	polyol reduction technique using an ultrasonic bath.	Fe_3O_4 particles (spherical shape aggregates) is ~73 nm. The primary particle size is ~16 nm.	The Ag layers were estimated at ~3.5, 9, and 11 nm for molar ratios of the ethanolic Ag solution to butylamine of 1:0.5, 1:1, and 1:2, respectively.	Magnetic saturation of Fe_3O_4: 91 emu/g.	[57]

Table 2. *Cont.*

Type of Core–Shell Material	Synthesis Conditions	Core Diameter	Shell Thickness	Properties	Reference
Fe_3O_4–Ag	Micro-emulsion method.	6 nm.	1.5 nm, 2 nm, and 8 nm.	Magnetic saturation: 55 emu/g for 1.5 nm Ag shell thickness; 53 emu/g for 2 nm Ag shell thickness. Nanocrystals with thicker nano-shells exhibit super-paramagnetic properties.	[62]
Fe_3O_4–Ag	Green synthesis, eco-friendly method.	The mean crystallite size of Fe_3O_4: 32 nm (XRD).	Core–shell particle size <50 nm (TEM).	ferromagnetic behavior; saturation magnetization (Ms) 15.74 emu/g.	[63]
Fe_3O_4–Au	Mild chemical synthesis (90 °C).	-	Core–shell size: ~9 nm.	Core–shell magnetic saturation (Ms): 42 emu/g. Ms = 46 emu/g for Fe_3O_4 core.	[71]
Fe_3O_4–Au	Green synthesis method (autoclave 120 °C/20 min).	5.77 nm (HRTEM).	Core–shell size: 6.08 nm (HRTEM).	Core–shell nanoparticles show the inhibitory concentration $(IC)_{50}$ of 235 µg/mL against a colorectal cancer cell line, HT-29. High saturation magnetization (Ms): 45.06 emu/g.	[72]
Fe_3O_4–SiO_2	In situ co-precipitation.	The average size of Fe_3O_4 core: 24 nm.	Mean thickness of SiO_2 shell: 18 nm.	Superparamagnetic properties. Saturation magnetization = 66 emu/g for Fe_3O_4 and 45 emu/g for Fe_3O_4/SiO_2.	[73]
Fe_3O_4–SiO_2	Chemical synthesis.	Mean diameter of Fe_3O_4 core: 10 ± 3 nm.	SiO_2 shell thickness: 35 ± 5 nm. the Fe_3O_4–SiO_2 core–shell thickness: 80 ± 5 nm).	Saturation magnetization values (Ms): 61.2 emu/g for Fe_3O_4, and 18.4 emu/g for Fe_3O_4–SiO_2.	[75]
Fe_3O_4–SiO_2	Mechanical mixing followed by sonication (modified Stöber techniques).	Average particle size of Fe_3O_4: 11.3 nm (TEM).	SiO_2 thickness: 4 nm (TEM). Average crystallite size of core–shell structure: 18 nm.	Optical conductivity of Fe_3O_4–SiO_2 nanoparticles has the highest value (24.4 eV^2) compared to the others.	[78]
Fe_3O_4–TiO_2	Hydro-thermal synthesis 200 °C/18 h.	Rod-shaped morphology. diameter of the core–shell structure was ~18 nm; length ~70 nm.		The magnetic saturation value of one sample was 1.27, 5.51 and 12.75 emu/g for T = 300, 100 and 15 K.	[43]
Fe_3O_4–TiO_2	Modified sol–gel method.	Diameter of Fe_3O_4 core: 7 nm.	TiO_2 thickness: 5 nm.	Ms = 55 emu/g for Fe_3O_4 (at 300 K) and 20 emu/g (at 300 K) for Fe_3O_4–TiO_2.	[83]
Fe_3O_4–TiO_2	Hydro-thermal method at 220 °C/24 h.	Crystal size of Fe_3O_4–TiO_2 varies between 8.14 nm (with oleic acid surfactant) and 34.85 nm (PEG surfactant).		Ms = 74.268 emu/g for Fe_3O_4 and 8.178 emu/g for Fe_3O_4–TiO_2.	[84]
Fe_3O_4–ZnO	Hydro-thermal synthesis 250 °C/30 min, N_2 atmosphere.	The average size of Fe_3O_4–ZnO: 10 nm (TEM).		Superparamagnetic behavior. Ms = 31.2 emu/g.	[33]
Fe_3O_4–ZnO	Microwave thermal treatment.	Spherical Fe_3O_4 core, diameter = 5 nm.	Spherical and rod-like ZnO shells with ~30 nm diameter and rod lengths ~70 nm.	Core–shell structures inhibit the growth of Gram-positive (*S. aureus*) and Gram-negative (*H. pylori*) pathogenic bacteria of clinical relevance.	[85]
Fe_3O_4–ZnO	Hydrothermal method, 200 °C/18 h.	The average crystallite size of Fe_3O_4–ZnO: 24 nm (molar ratio 1:5), 20 nm (1:10), and 18 nm (1:20 nm).		Only the lowest concentrations of Fe_3O_4–ZnO Core–shell nanoparticles are appropriate for biomedical applications.	[87]
Fe_3O_4–ZnO	Hydro-thermal method, 170 °C/10 h.	7 nm.	60 nm.	The magnetization saturation value of the core–shell nanoparticles is 5.96 emu/g.	[92]

Table 2. *Cont.*

Type of Core–Shell Material	Synthesis Conditions	Core Diameter	Shell Thickness	Properties	Reference
Fe_3O_4–chitosan–Ag	Suspension technique.	-	-	Ms = 60.06 emu/g for pure Fe_3O_4; 40.39 emu/g for Fe_3O_4–chitosan and 46.72 emu/g for Fe_3O_4–chitosan–Ag bacterial and fungi inhibitors. 99.5% prevention of the growth of microorganisms. 100% inhibition rate of *E. coli* and *S. cerevisiae*.	[100]
Fe_3O_4–heparine–poloxamer (HP)	Ultra-sonication 6 h, room temperature.	The average size of Fe_3O_4 is 11.6 nm (from TEM).	The average size of Fe_3O_4–HP is 17.7 nm (from TEM).	Ms = 24.92 emu/g for core–shell structures. Ms = 68.9 emu/g for Fe_3O_4. DOX-loaded Fe_3O_4–HP showed a great anticancer effect against HeLa cells. Loading efficiency of DOX into Fe_3O_4–HP was 66.9 ±2.7%. controlled release up to 120 h without any initial burst effect.	[98]
Fe_3O_4–PNIPAAm	Polymerization of NIPAAm in the presence of Fe_3O_4 at 90 °C for 5 days, followed by dialysis. The monomer conversion was about 70%.	20 nm	Spherical particle size of 40 nm in diameter for Fe_3O_4–PNIPAAm nanoparticles. shell thickness: 10–15 nm.	Anticancer drugs. The highest release percentage of methotrexate (MTX) has been observed at pH = 5.5 and 40 °C. MTX was better for lung cancer than for breast cancer.	[32]

3. Conclusions and Perspectives

Core–shell nanoparticles are an important class of materials for biomedical applications. This mini-review has been focused on nanoparticles having Fe_3O_4 as a core and various types of shells, especially inorganic ones. It has been shown that medical applications of these nanostructures depend on their size, shape, and properties. The most common morphology is spherically shaped nanoparticles. The most efficient particle sizes seem to be in the range of 6–50 nm.

In some cases, the shell thickness was higher than the core diameter, leading to a decrease in magnetic saturation value, which affects its use as a contrast agent (MRI contrast ability is lower).

Generally, the most suitable nanoparticles for cancer therapy are those with diameters between 10 and 100 nm. Particles with around 10 nm diameter have a higher surface area-to-volume ratio and are more effective for drug delivery and imaging, while particles with approximately 50 nm diameter may be more effective in hyperthermia treatment.

Too small particles (less than 2 nm) can easily leak from the normal vasculature, and particles below 10 nm can be filtered by the kidneys. Particles larger than 100 nm can be cleared from circulation by phagocytes.

Fe_3O_4 core–shell nanoparticles are still under development regarding their use as magnetic contrast agents, hyperthermia agents, or drug delivery systems in clinical applications on human patients. It is necessary to investigate and understand the interaction between core –shell nanoparticles and human tissues before clinical trials.

In hyperthermia, the damaged body tissue is exposed to high temperatures in order to damage and kill cancer cells or make them more sensitive to radiation and anticancer drugs. In magnetic hyperthermia, an external magnetic field is used to control magnetic nanoparticles, which are introduced into the human body through intravenous injection, intratumoral injection, or targeted delivery to damaged organs or tissues. Fe_3O_4 nanoparticles absorb electromagnetic energy and convert it into heat (>41.5 °C). The inductive heating effect of iron oxide nanoparticles appears when an alternating magnetic field suddenly changes the magnetic orientation of the superparamagnetic magnetite particles. Rapid

alternation of the magnetic orientation produces particle vibration and further generates heat after internalization, causing cell death when temperatures reach approximately 42 °C. The heat generated by the magnetic nanoparticles can kill cancer cells without damaging healthy tissue.

Another method to treat cancer using Fe_3O_4 core–shell nanoparticles is to apply mechanical pressure to cancer cells in order to cause magnetic particle vibrations, which will finally cause cell death.

Targeted cancer therapies are developed to interrupt the uncontrolled proliferation of cancer cells. Core–shell nanoparticles can be designed to deliver drugs only after entering the tumor tissues. This could reduce side effects and increase the accuracy of tumor targeting with improved treatment efficacy. Fe_3O_4 core–shell nanoparticles present various reactive sites for contact with drugs and can be triggered for binding to specific sites, release the drug at a certain time/temperature/pH, in a controlled manner (shell thickness dependent, ROS-mediated cytotoxicity, microwave-triggered), etc. The drugs embedded in core–shell nanostructures accumulate in cancer cells under the influence of the external magnetic field through enhanced permeability and retention effects.

For nanoparticles, as in the case of medicines, in parallel with the effectiveness, the safety of use is also evaluated. Over the past 40 years, the number and variety of controlled-release drug delivery systems have greatly increased, but despite all the successes achieved, the delivery systems have not been fully accepted due to issues with the regulatory process. Many of the nanoformulations of oncology drugs were retracted from the market, although they had already received Food and Drug Administration (FDA) approval. Newly investigated therapeutic nanoparticles with anticancer properties have some limitations and fail to pass clinical trials. The major drawback is the lack of understanding of the mechanism of nanoparticles' interaction with biomolecules in the human body. Other important limitations are cellular internalization of the drug (heterogeneous accumulation in the tumor cells). Less than 1% of injected nanoparticles reach the tumor because of the complexity of the tumor; drug release rate; nanoparticles should remain in circulation long enough to allow for significant tumor accumulation; drugs should not be dispersed and distributed in the entire body; nanoparticles that serve as drug nanocarriers should be capable of targeting only tumor cells; and the prediction of the response of the immune system to the newly introduced nanoparticles in the human body tissues.

Researchers are investigating the possibility of creating multifunctional nanoparticles that, after detecting the tumor in the body, can also proceed to its treatment, a fact that would revolutionize oncological practice, replacing the classical therapeutic methods such as chemotherapy and radiotherapy that affect not only cancer cells but also those healthy, destroying them. With the help of nanotechnologies, cancer cells could be destroyed in a targeted manner without harming healthy tissue in any way.

It is necessary to enhance the selectivity and accuracy of delivery for core–shell nanoparticles to target cancer cells. The major challenges are to design nanoparticles that are stable in the patient's bloodstream and possess improved precision and efficacy for the therapeutic treatment of tumors. Consequently, there is a need to improve synthesis methods to obtain new core–shell nanoparticles for local control of tumors and improved targeted delivery of agents for cancer therapy. Among the synthesis methods briefly presented in this review, hydrothermal synthesis of Fe_3O_4 core–shell nanoparticles combined with phyto-synthesis of one component (either magnetite or shell) using different plant extracts is eco-friendly, cost-effective, and can ensure control of particle size and morphology for tailored applications (drug delivery nanocarriers or magnetic hyperthermia therapy).

In the future, it should be used under mild synthesis conditions of the hydrothermal method: A shorter reaction time ($\leq$3 h) and lower temperature ($\leq$200 °C) coupled with supplementary pressure (from an external source through inert gas bubbling such as Ar or N_2) created in addition to the vapor pressure formed above the reaction system could lead to core–shell nanoparticles with improved properties. Inorganic core–shell precursors such as

chloride, nitrate, and sulfate are cheaper than organic–metallic ones and should be further used to avoid any environmental problems created by organic solvents or precursors.

Future research should focus on biological, technological, and design aspects regarding the use of Fe_3O_4 core–shell nanoparticles in cancer treatment. Thus, biological aspects refer to the interactions of core–shell nanostructures in the human body with living cells, organs, and species. An important issue to be solved in the future is what happens with insoluble or very little soluble nondegradable nanoparticles in the human body. Moreover, the linkage between drug-loaded nanoparticles and cells should be studied to understand the mechanism of cellular uptake. Technological aspects refer to scale-up synthesis and performance predictions. It should be possible to find cost-effective synthesis routes capable of yielding large quantities of chemicals that can be produced by pharmaceutical companies. Currently, predicting nanoparticle efficacy and performance in real human tissues is hard because nanoparticle therapy is applied to patients after several classical routes (surgery, chemotherapy, phototherapy, and radiation therapy) have been administered and their immune systems have already been affected by the respective treatment. Computational or theoretical modeling, along with experimental results, can be designed to imitate physiological tissue and the surrounding environment or to study the interaction between drug carriers and cells. The design of drug nanocarriers based on core–shell nanostructures should consider colloidal stability, drug loading capacity, tracking, the release of drug components only at the target sites, biocompatibility, toxicity, and minimal risk (to avoid spreading or accumulation of the drug in other tissues or organs). The particle sizes and size distributions must be reproducible. Fighting cancer is an old dream of physicians and researchers, and it makes them confident that one day the cure for this disease will be discovered.

Author Contributions: Conceptualization, L.-M.C. and A.-G.Ș.; literature search—M.-A.I.; writing—original draft preparation, M.-A.I.; writing—review and editing, L.-M.C. and A.-M.M.; supervision, R.M.P. and A.-G.Ș.; project administration, I.A.T.; funding acquisition, A.-M.M. All authors have read and agreed to the published version of the manuscript.

Funding: This research was funded by MCID, project no. 23250202, through the Core Program within the National Research Development and Innovation Plan 2022–2027 and INOVADIT project of the Ministry of Research, Innovation, and Digitization through Program 1—Development of the national research-development system, Subprogram 1.2-Institutional performance-Projects for financing excellence in RDI, Contract no. 9PFE/2021.

Data Availability Statement: No new data were created or analyzed in this study. Data sharing is not applicable to this article.

Acknowledgments: This work was performed through the Core Program within the National Research Development and Innovation Plan 2022–2027, carried out with the support of MCID, project no. 23250202, and the INOVADIT project of the Ministry of Research, Innovation, and Digitization through Program 1—Development of the national research-development system, Subprogram 1.2—Institutional Performance-Projects for Financing Excellence in RDI, Contract no. 9PFE/2021. M.-A. Ioța and A.-G. Șchiopu gratefully acknowledge the Interdisciplinary Doctoral School, University of Pitești, for administrative and technical support.

Conflicts of Interest: The authors declare no conflict of interest. The funders had no role in the design of the study; in the collection, analyses, or interpretation of data; in the writing of the manuscript; or in the decision to publish the results.

References

1. Musielak, M.; Piotrowski, I.; Suchorska, W.M. Superparamagnetic Iron Oxide Nanoparticles (SPIONs) as a Multifunctional Tool in Various Cancer Therapies. *Rep. Pract. Oncol. Radiother.* **2019**, *24*, 307–314. [CrossRef] [PubMed]
2. Shen, L.; Li, B.; Qiao, Y. Fe_3O_4 Nanoparticles in Targeted Drug/Gene Delivery Systems. *Materials* **2018**, *11*, 324. [CrossRef] [PubMed]
3. Liu, S.; Yu, B.; Wang, S.; Shen, Y.; Cong, H. Preparation, Surface Functionalization and Application of Fe_3O_4 Magnetic Nanoparticles. *Adv. Colloid Interface Sci.* **2020**, *281*, 102165. [CrossRef] [PubMed]

4. Laurent, S.; Saei, A.A.; Behzadi, S.; Panahifar, A.; Mahmoudi, M. Superparamagnetic Iron Oxide Nanoparticles for Delivery of Therapeutic Agents: Opportunities and Challenges. *Expert Opin. Drug Deliv.* **2014**, *11*, 1449–1470. [CrossRef]
5. Shaw, S.K.; Sharma, A.; Kailashiya, J.; Gupta, S.K.; Meena, S.S.; Dash, D.; Maiti, P.; Prasad, N.K. Mesoporous Fe_3O_4 Nanoparticle: A Prospective Nano Heat Generator for Thermo-Therapeutic Cancer Treatment Modality. *J. Magn. Magn. Mater.* **2023**, *578*, 170817. [CrossRef]
6. Shubitidze, F.; Kekalo, K.; Stigliano, R.; Baker, I. Magnetic Nanoparticles with High Specific Absorption Rate of Electromagnetic Energy at Low Field Strength for Hyperthermia Therapy. *J. Appl. Phys.* **2015**, *117*, 094302. [CrossRef]
7. Yew, Y.P.; Shameli, K.; Miyake, M.; Ahmad Khairudin, N.B.B.; Mohamad, S.E.B.; Naiki, T.; Lee, K.X. Green Biosynthesis of Superparamagnetic Magnetite Fe_3O_4 Nanoparticles and Biomedical Applications in Targeted Anticancer Drug Delivery System: A Review. *Arab. J. Chem.* **2020**, *13*, 2287–2308. [CrossRef]
8. Fu, S.; Wang, S.; Zhang, X.; Qi, A.; Liu, Z.; Yu, X.; Chen, C.; Li, L. Structural Effect of Fe_3O_4 Nanoparticles on Peroxidase-like Activity for Cancer Therapy. *Colloids Surf. B Biointerfaces* **2017**, *154*, 239–245. [CrossRef]
9. Xie, J.; Liu, G.; Eden, H.S.; Ai, H.; Chen, X. Surface-Engineered Magnetic Nanoparticle Platforms for Cancer Imaging and Therapy. *Acc. Chem. Res.* **2011**, *44*, 883–892. [CrossRef]
10. Gao, Z.; Ma, T.; Zhao, E.; Docter, D.; Yang, W.; Stauber, R.H.; Gao, M. Small Is Smarter: Nano MRI Contrast Agents—Advantages and Recent Achievements. *Small* **2016**, *12*, 556–576. [CrossRef]
11. Ulbrich, K.; Holá, K.; Šubr, V.; Bakandritsos, A.; Tuček, J.; Zbořil, R. Targeted Drug Delivery with Polymers and Magnetic Nanoparticles: Covalent and Noncovalent Approaches, Release Control, and Clinical Studies. *Chem. Rev.* **2016**, *116*, 5338–5431. [CrossRef]
12. Datta, N.R.; Krishnan, S.; Speiser, D.E.; Neufeld, E.; Kuster, N.; Bodis, S.; Hofmann, H. Magnetic Nanoparticle-Induced Hyperthermia with Appropriate Payloads: Paul Ehrlich's "Magic (Nano)Bullet" for Cancer Theranostics? *Cancer Treat Rev.* **2016**, *50*, 217–227. [CrossRef]
13. Beik, J.; Abed, Z.; Ghoreishi, F.S.; Hosseini-Nami, S.; Mehrzadi, S.; Shakeri-Zadeh, A.; Kamrava, S.K. Nanotechnology in Hyperthermia Cancer Therapy: From Fundamental Principles to Advanced Applications. *J. Control. Release* **2016**, *235*, 205–221. [CrossRef]
14. Kaewsaneha, C.; Tangboriboonrat, P.; Polpanich, D.; Elaissari, A. Multifunctional Fluorescent-Magnetic Polymeric Colloidal Particles: Preparations and Bioanalytical Applications. *ACS Appl. Mater. Interfaces* **2015**, *7*, 23373–23386. [CrossRef]
15. Sahadevan, J.; Sojiya, R.; Padmanathan, N.; Kulathuraan, K.; Shalini, M.G.; Sivaprakash, P.; Esakki Muthu, S. Magnetic Property of Fe_2O_3 and Fe_3O_4 Nanoparticle Prepared by Solvothermal Process. *Mater. Today Proc.* **2022**, *58*, 895–897. [CrossRef]
16. Chomoucka, J.; Drbohlavova, J.; Huska, D.; Adam, V.; Kizek, R.; Hubalek, J. Magnetic Nanoparticles and Targeted Drug Delivering. *Pharmacol. Res.* **2010**, *62*, 144–149. [CrossRef]
17. Tartaj, P.; Morales, M.P.; González-Carreño, T.; Veintemillas-Verdaguer, S.; Serna, C.J. Advances in Magnetic Nanoparticles for Biotechnology Applications. *J. Magn. Magn. Mater.* **2005**, *290–291 Pt 1*, 28–34. [CrossRef]
18. Majewski, P.; Thierry, B. Functionalized Magnetite Nanoparticles—Synthesis, Properties, and Bio-Applications. *Crit. Rev. Solid State Mater. Sci.* **2007**, *32*, 203–215. [CrossRef]
19. Neuberger, T.; Schöpf, B.; Hofmann, H.; Hofmann, M.; Von Rechenberg, B. Superparamagnetic Nanoparticles for Biomedical Applications: Possibilities and Limitations of a New Drug Delivery System. *J. Magn. Magn. Mater.* **2005**, *293*, 483–496. [CrossRef]
20. Mona, L.P.; Songca, S.P.; Ajibade, P.A. Synthesis and Encapsulation of Iron Oxidenanorods for Application in Magnetichyperthermia and Photothermal Therapy. *Nanotechnol. Rev.* **2022**, *11*, 176–190. [CrossRef]
21. Thomas, R.; Park, I.K.; Jeong, Y.Y. Magnetic Iron Oxide Nanoparticles for Multimodal Imaging and Therapy of Cancer. *Int. J. Mol. Sci.* **2013**, *14*, 15910–15930. [CrossRef] [PubMed]
22. Estelrich, J.; Sánchez-Martín, M.J.; Busquets, M.A. Nanoparticles in Magnetic Resonance Imaging. Rom Simple to Dual Contrast Agents. *Int. J. Nanomed.* **2015**, *10*, 1727–1741.
23. Kim, J.; Piao, Y.; Hyeon, T. Multifunctional Nanostructured Materials for Multimodal Imaging, and Simultaneous Imaging and Therapy. *Chem. Soc. Rev.* **2009**, *38*, 372–390. [CrossRef] [PubMed]
24. Govindan, B.; Sabri, M.A.; Hai, A.; Banat, F.; Haija, M.A. A Review of Advanced Multifunctional Magnetic Nanostructures for Cancer Diagnosis and Therapy Integrated into an Artificial Intelligence Approach. *Pharmaceutics* **2023**, *15*, 868. [CrossRef] [PubMed]
25. Olusegun, S.J.; Osial, M.; Majkowska-Pilip, A.; Żelechowska-Matysiak, K.; Nieciecka, D.; Krajewski, M.; Pękała, M.; Krysinski, P. Synthesis and Characterization of Sr^{2+} and Gd^{3+} Doped Magnetite Nanoparticles for Magnetic Hyperthermia and Drug Delivery Application. *Ceram. Int.* **2023**, *49*, 19851–19860. [CrossRef]
26. Revia, R.A.; Zhang, M. Magnetite Nanoparticles for Cancer Diagnosis, Treatment, and Treatment Monitoring: Recent Advances. *Mater. Today* **2016**, *19*, 157–168. [CrossRef]
27. Nuzhina, J.V.; Shtil, A.A.; Prilepskii, A.Y.; Vinogradov, V.V. Preclinical Evaluation and Clinical Translation of Magnetite-Based Nanomedicines. *J. Drug Deliv. Sci. Technol.* **2019**, *54*, 101282. [CrossRef]
28. Attia, N.F.; El-Monaem, E.M.A.; El-Aqapa, H.G.; Elashery, S.E.A.; Eltaweil, A.S.; El Kady, M.; Khalifa, S.A.M.; Hawash, H.B.; El-Seedi, H.R. Iron Oxide Nanoparticles and Their Pharmaceutical Applications. *Appl. Surf. Sci. Adv.* **2022**, *11*, 100284. [CrossRef]
29. Alamdari, S.G.; Amini, M.; Jalilzadeh, N.; Baradaran, B.; Mohammadzadeh, R.; Mokhtarzadeh, A.; Oroojalian, F. Recent Advances in Nanoparticle-Based Photothermal Therapy for Breast Cancer. *J. Control. Release* **2022**, *349*, 269–303. [CrossRef]

30. Rodrigues, G.R.; López-Abarrategui, C.; de la Serna Gómez, I.; Dias, S.C.; Otero-González, A.J.; Franco, O.L. Antimicrobial Magnetic Nanoparticles Based-Therapies for Controlling Infectious Diseases. *Int. J. Pharm.* **2019**, *555*, 356–367. [CrossRef]
31. Nieciecka, D.; Celej, J.; Żuk, M.; Majkowska-pilip, A.; Żelechowska-Matysiak, K.; Lis, A.; Osial, M. Hybrid System for Local Drug Delivery and Magnetic Hyperthermia Based on Spions Loaded with Doxorubicin and Epirubicin. *Pharmaceutics* **2021**, *13*, 480. [CrossRef]
32. Moradi, S.; Najjar, R.; Hamishehkar, H.; Lotfi, A. Triple-Responsive Drug Nanocarrier: Magnetic Core-Shell Nanoparticles of Fe_3O_4@poly(N-Isopropylacrylamide)-Grafted-Chitosan, Synthesis and In Vitro Cytotoxicity Evaluation against Human Lung and Breast Cancer Cells. *J. Drug Deliv. Sci. Technol.* **2022**, *72*, 103426. [CrossRef]
33. Gupta, J.; Hassan, P.A.; Barick, K.C. Core-Shell Fe_3O_4@ZnO Nanoparticles for Magnetic Hyperthermia and Bio-Imaging Applications. *AIP Adv.* **2021**, *11*, 025207. [CrossRef]
34. Rybka, J.D. Radiosensitizing Properties of Magnetic Hyperthermia Mediated by Superparamagnetic Iron Oxide Nanoparticles (SPIONs) on Human Cutaneous Melanoma Cell Lines. *Rep. Pract. Oncol. Radiother.* **2019**, *24*, 152–157. [CrossRef]
35. Katifelis, H.; Mukha, I.; Lyberopoulou, A.; Vityuk, N.; Grammatikaki, M.; Pylypchuk, I.; Lazaris, F.; Storozhuk, L.; Kouloulias, V.; Gazouli, M. In Vitro Effect of Hyperthermic Ag and Au Fe_3O_4 Nanoparticles in Cancer Cells. *Beilstein Arch.* **2019**, 2019101. [CrossRef]
36. Liu, L.; Li, Y.; Abdulkreem AL-Huqail, A.; Ali, E.; Alkhalifah, T.; Alturise, F.; Ali, H.E. Green Synthesis of Fe_3O_4 Nanoparticles Using Alliaceae Waste (*Allium sativum*) for a Sustainable Landscape Enhancement Using Support Vector Regression. *Chemosphere* **2023**, *334*, 138638. [CrossRef]
37. Roy, S.; Hasan, I.; Guo, B. Recent Advances in Nanoparticle-Mediated Antibacterial Applications. *Coord. Chem. Rev.* **2023**, *482*, 215075. [CrossRef]
38. Singh, M.; Savchenko, A.; Shetinin, I.; Majouga, A. An Original Route to Target Delivery via Core-Shell Modification. *Mater. Today Proc.* **2016**, *3*, 2652–2661. [CrossRef]
39. Mélinon, P.; Begin-Colin, S.; Duvail, J.L.; Gauffre, F.; Boime, N.H.; Ledoux, G.; Plain, J.; Reiss, P.; Silly, F.; Warot-Fonrose, B. Engineered Inorganic Core/Shell Nanoparticles. *Phys. Rep.* **2014**, *543*, 163–197. [CrossRef]
40. Sun, Z.; Zhou, X.; Luo, W.; Yue, Q.; Zhang, Y.; Cheng, X.; Li, W.; Kong, B.; Deng, Y.; Zhao, D. Interfacial Engineering of Magnetic Particles with Porous Shells: Towards Magnetic Core–Porous Shell Microparticles. *Nano Today* **2016**, *11*, 464–482. [CrossRef]
41. Su, H.; Tian, Q.; Hurd Price, C.A.; Xu, L.; Qian, K.; Liu, J. Nanoporous Core@shell Particles: Design, Preparation, Applications in Bioadsorption and Biocatalysis. *Nano Today* **2020**, *31*, 100834. [CrossRef]
42. Ren, Q.; Yi, C.; Pan, J.; Sun, X.; Huang, X. Smart Fe_3O_4@ZnO Core-Shell Nanophotosensitizers Potential for Combined Chemo and Photodynamic Skin Cancer Therapy Controlled by UVA Radiation. *Int. J. Nanomed.* **2022**, *17*, 3385–3400. [CrossRef] [PubMed]
43. Madhubala, V.; Nagarajan, C.; Baskaran, P.; Raguraman, V.; Kalaivani, T. Formulation of Magnetic Core-Shell Nanostructured Fe_3O_4@TiO_2 for Cytotoxic Activity against Huh-7 Cells. *Inorg. Chem. Commun.* **2023**, *149*, 110430. [CrossRef]
44. Madhubala, V.; Nagarajan, C.; Baskaran, P.; Raguraman, V.; Kalaivani, T. Influences of Superparamagnetic Fe_3O_4@Ag Core-Shell Nanoparticles on the Growth Inhibition of Huh-7 Cells. *Mater. Today Commun.* **2023**, *35*, 106139. [CrossRef]
45. Izadiyan, Z.; Shameli, K.; Teow, S.Y.; Yusefi, M.; Kia, P.; Rasouli, E.; Tareq, M.A. Anticancer Activity of 5-Fluorouracil-Loaded Nanoemulsions Containing Fe_3O_4/Au Core-Shell Nanoparticles. *J. Mol. Struct.* **2021**, *1245*, 131075. [CrossRef]
46. Sánchez-Orozco, J.L.; García-Cerda, L.A.; Puente-Urbina, B.; Meléndez-Ortiz, H.I. Poly(N-Vinylcaprolactam-Co-2-(Diethylamino) Ethylmethacrylate) Coated Fe_3O_4@SiO_2 Core-Shell Magnetic Nanoparticles for Controlled Doxorubicin Delivery. *J. Drug Deliv. Sci. Technol.* **2023**, *81*, 104253. [CrossRef]
47. Gupta, A.K.; Gupta, M. Synthesis and Surface Engineering of Iron Oxide Nanoparticles for Biomedical Applications. *Biomaterials* **2005**, *26*, 3995–4021. [CrossRef]
48. Yeneayehu, K.; Senbeta, T.; Mesfin, B. Enhancement of the Optical Response of Fe_3O_4@Ag Core-Shell Nanoparticles. *Phys. E Low Dimens. Syst. Nanostruct.* **2021**, *134*, 114822. [CrossRef]
49. Díez, A.G.; Rincón-Iglesias, M.; Lanceros-Méndez, S.; Reguera, J.; Lizundia, E. Multicomponent Magnetic Nanoparticle Engineering: The Role of Structure-Property Relationship in Advanced Applications. *Mater. Today Chem.* **2022**, *26*, 101220. [CrossRef]
50. Khatami, M.; Alijani, H.Q.; Nejad, M.S.; Varma, R.S. Core@shell Nanoparticles: Greener Synthesis Using Natural Plant Products. *Appl. Sci.* **2018**, *8*, 411. [CrossRef]
51. Azizabadi, O.; Akbarzadeh, F.; Danshina, S.; Chauhan, N.P.S.; Sargazi, G. An Efficient Ultrasonic Assisted Reverse Micelle Synthesis Route for Fe_3O_4@Cu-MOF/Core-Shell Nanostructures and Its Antibacterial Activities. *J. Solid State Chem.* **2021**, *294*, 121897. [CrossRef]
52. Sun, Y.; Tian, Y.; He, M.; Zhao, Q.; Chen, C.; Hu, C.; Liu, Y. Controlled Synthesis of Fe_3O_4/Ag Core-Shell Composite Nanoparticles with High Electrical Conductivity. *J. Electron. Mater.* **2012**, *41*, 519–523. [CrossRef]
53. Amarjargal, A.; Tijing, L.D.; Im, I.T.; Kim, C.S. Simultaneous Preparation of Ag/Fe_3O_4 Core-Shell Nanocomposites with Enhanced Magnetic Moment and Strong Antibacterial and Catalytic Properties. *Chem. Eng. J.* **2013**, *226*, 243–254. [CrossRef]
54. Iglesias-Silva, E.; Rivas, J.; León Isidro, L.M.; López-Quintela, M.A. Synthesis of Silver-Coated Magnetite Nanoparticles. *J. Non-Cryst. Solids* **2007**, *353*, 829–831. [CrossRef]
55. Mandal, M.; Kundu, S.; Ghosh, S.K.; Panigrahi, S.; Sau, T.K.; Yusuf, S.M.; Pal, T. Magnetite Nanoparticles with Tunable Gold or Silver Shell. *J. Colloid Interface Sci.* **2005**, *286*, 187–194. [CrossRef]

56. Kalska-Szostko, B.; Wykowska, U.; Satuła, D. Magnetic Nanoparticles of Core-Shell Structure. *Colloids Surf. A Physicochem. Eng. Asp.* **2015**, *481*, 527–536. [CrossRef]
57. Ghazanfari, M.; Johar, F.; Yazdani, A. Synthesis and Characterization of Fe_3O_4 @Ag Core-Shell: Structural, Morphological, and Magnetic Properties. *J. Ultrafine Grained Nanostruct. Mater.* **2014**, *47*, 97–103.
58. Brollo, M.E.F.; López-Ruiz, R.; Muraca, D.; Figueroa, S.J.A.; Pirota, K.R.; Knobel, M. Compact Ag@Fe_3O_4 Core-Shell Nanoparticles by Means of Single-Step Thermal Decomposition Reaction. *Sci. Rep.* **2014**, *4*, 6839. [CrossRef]
59. Dehghan, Z.; Ranjbar, M.; Govahi, M.; Khakdan, F. Green Synthesis of Ag/Fe_3O_4 Nanocomposite Utilizing Eryngium Planum L. Leaf Extract and Its Potential Applications in Medicine. *J. Drug Deliv. Sci. Technol.* **2022**, *67*, 102941. [CrossRef]
60. Ding, Q.; Liu, D.; Guo, D.; Yang, F.; Pang, X.; Che, R.; Zhou, N.; Xie, J.; Sun, J.; Huang, Z.; et al. Shape-Controlled Fabrication of Magnetite Silver Hybrid Nanoparticles with High Performance Magnetic Hyperthermia. *Biomaterials* **2017**, *124*, 35–46. [CrossRef]
61. Nguyen-Tri, P.; Nguyen, V.T.; Nguyen, T.A. Biological Activity and Nanostructuration of Fe_3O_4-Ag/High Density Polyethylene Nanocomposites. *J. Compos. Sci.* **2019**, *3*, 34. [CrossRef]
62. Singh, P.; Upadhyay, C. Role of Silver Nanoshells on Structural and Magnetic Behavior of Fe_3O_4 Nanoparticles. *J. Magn. Magn. Mater.* **2018**, *458*, 39–47. [CrossRef]
63. Venkateswarlu, S.; Natesh Kumar, B.; Prathima, B.; Anitha, K.; Jyothi, N.V.V. A Novel Green Synthesis of Fe_3O_4-Ag Core Shell Recyclable Nanoparticles Using Vitis Vinifera Stem Extract and Its Enhanced Antibacterial Performance. *Phys. B Condens. Matter* **2015**, *457*, 30–35. [CrossRef]
64. Sajjadi, M.; Nasrollahzadeh, M.; Mohammad Sajadi, S. Green Synthesis of Ag/Fe_3O_4 Nanocomposite Using Euphorbia Peplus Linn Leaf Extract and Evaluation of Its Catalytic Activity. *J. Colloid Interface Sci.* **2017**, *497*, 1–13. [CrossRef]
65. Danafar, H.; Baghdadchi, Y.; Barsbay, M.; Ghaffarlou, M.; Mousazadeh, N.; Mohammadi, A. Synthesis of Fe_3O_4-Gold Hybrid Nanoparticles Coated by Bovine Serum Albumin as a Contrast Agent in MR Imaging. *Heliyon* **2023**, *9*, e13874. [CrossRef]
66. Aydın, E.B.; Aydın, M.; Sezgintürk, M.K. Determination of Calreticulin Using Fe_3O_4@AuNPs Core-Shell Functionalized with $PT(COOH)_2$ Polymer Modified Electrode: A New Platform for the Impedimetric Biosensing of Cancer Biomarkers. *Sens. Actuators B Chem.* **2022**, *367*, 132099. [CrossRef]
67. Tarhan, T.; Ulu, A.; Sariçam, M.; Çulha, M.; Ates, B. Maltose Functionalized Magnetic Core/Shell Fe_3O_4@Au Nanoparticles for an Efficient L-Asparaginase Immobilization. *Int. J. Biol. Macromol.* **2020**, *142*, 443–451. [CrossRef]
68. Wang, W.; Luo, J.; Fan, Q.; Suzuki, M.; Suzuki, I.S.; Engelhard, M.H.; Lin, Y.; Kim, N.; Wang, J.Q.; Zhong, C.J. Monodispersed Core-Shell Fe_3O_4@Au Nanoparticles. *J. Phys. Chem. B* **2005**, *109*, 21593–21601. [CrossRef]
69. Chatterjee, K.; Sarkar, S.; Jagajjanani Rao, K.; Paria, S. Core/Shell Nanoparticles in Biomedical Applications. *Adv. Colloid Interface Sci.* **2014**, *209*, 8–39. [CrossRef]
70. Salihov, S.V.; Ivanenkov, Y.A.; Krechetov, S.P.; Veselov, M.S.; Sviridenkova, N.V.; Savchenko, A.G.; Klyachko, N.L.; Golovin, Y.I.; Chufarova, N.V.; Beloglazkina, E.K.; et al. Recent Advances in the Synthesis of Fe_3O_4@AU Core/Shell Nanoparticles. *J. Magn. Magn. Mater.* **2015**, *394*, 173–178. [CrossRef]
71. Rajkumar, S.; Prabaharan, M. Multi-Functional Core-Shell Fe_3O_4@Au Nanoparticles for Cancer Diagnosis and Therapy. *Colloids Surf. B Biointerfaces* **2019**, *174*, 252–259. [CrossRef]
72. Izadiyan, Z.; Shameli, K.; Miyake, M.; Teow, S.Y.; Peh, S.C.; Mohamad, S.E.; Mohd Taib, S.H. Green Fabrication of Biologically Active Magnetic Core-Shell Fe_3O_4/Au Nanoparticles and Their Potential Anticancer Effect. *Mater. Sci. Eng. C* **2019**, *96*, 51–57. [CrossRef]
73. Mostafaei, M.; Hosseini, S.N.; Khatami, M.; Javidanbardan, A.; Sepahy, A.A.; Asadi, E. Isolation of Recombinant Hepatitis B Surface Antigen with Antibody-Conjugated Superparamagnetic Fe_3O_4/SiO_2 Core-Shell Nanoparticles. *Protein Expr. Purif.* **2018**, *145*, 1–6. [CrossRef]
74. Shao, H.; Qi, J.; Lin, T.; Zhou, Y. Preparation and Characterization of Fe_3O_4@SiO_2@NMDP Core-Shell Structure Composite Magnetic Nanoparticles. *Ceram. Int.* **2018**, *44*, 2255–2260. [CrossRef]
75. Ta, T.K.H.; Trinh, M.T.; Long, N.V.; Nguyen, T.T.M.; Nguyen, T.L.T.; Thuoc, T.L.; Phan, B.T.; Mott, D.; Maenosono, S.; Tran-Van, H.; et al. Synthesis and Surface Functionalization of Fe_3O_4-SiO_2 Core-Shell Nanoparticles with 3-Glycidoxypropyltrimethoxysilane and 1,1′-Carbonyldiimidazole for Bio-Applications. *Colloids Surf. A Physicochem. Eng. Asp.* **2016**, *504*, 376–383. [CrossRef]
76. Santra, S.; Tapec, R.; Theodoropoulou, N.; Dobson, J.; Hebard, A.; Tan, W. Synthesis and Characterization of Silica-Coated Iron Oxide Nanoparticles in Microemulsion: The Effect of Nonionic Surfactants. *Langmuir* **2001**, *17*, 2900–2906. [CrossRef]
77. Tadyszak, K.; Kertmen, A.; Coy, E.; Andruszkiewicz, R.; Milewski, S.; Kardava, I.; Scheibe, B.; Jurga, S.; Chybczyńska, K. Spectroscopic and Magnetic Studies of Highly Dispersible Superparamagnetic Silica Coated Magnetite Nanoparticles. *J. Magn. Magn. Mater.* **2017**, *433*, 254–261. [CrossRef]
78. Khalid, A.; Ahmed, R.M.; Taha, M.; Soliman, T.S. Fe_3O_4 Nanoparticles and Fe_3O_4 @SiO_2 Core-Shell: Synthesize, Structural, Morphological, Linear, and Nonlinear Optical Properties. *J. Alloys Compd.* **2023**, *947*, 169639. [CrossRef]
79. Asgari, M.; Miri, T.; Soleymani, M.; Barati, A. A Novel Method for in Situ Encapsulation of Curcumin in Magnetite-Silica Core-Shell Nanocomposites: A Multifunctional Platform for Controlled Drug Delivery and Magnetic Hyperthermia Therapy. *J. Mol. Liq.* **2021**, *324*, 114731. [CrossRef]
80. Lu, C.H.; Chen, G.H.; Yu, B.; Cong, H.L.; Kong, L.M.; Guo, L. Design and Synthesis of Fe_3O_4@SiO_2 Core-Shell Nanomaterials. *Integr. Ferroelectr.* **2017**, *182*, 46–52. [CrossRef]
81. Chen, X.; Selloni, A. Introduction: Titanium Dioxide (TiO_2) Nanomaterials. *Chem. Rev.* **2014**, *114*, 9281–9282. [CrossRef] [PubMed]

82. Madhubala, V.; Pugazhendhi, A.; Thirunavukarasu, K. Cytotoxic and Immunomodulatory Effects of the Low Concentration of Titanium Dioxide Nanoparticles (TiO_2 NPs) on Human Cell Lines—An In Vitro Study. *Process Biochem.* **2019**, *86*, 186–195. [CrossRef]
83. Khashan, S.; Dagher, S.; Tit, N.; Alazzam, A.; Obaidat, I. Novel Method for Synthesis of Fe_3O_4@TiO_2 Core/Shell Nanoparticles. *Surf. Coat. Technol.* **2017**, *322*, 92–98. [CrossRef]
84. Rani, N.; Dehiya, B.S. Influence of Anionic and Non-Ionic Surfactants on the Synthesis of Core-Shell Fe_3O_4@TiO_2 Nanocomposite Synthesized by Hydrothermal Method. *Ceram. Int.* **2020**, *46*, 23516–23525. [CrossRef]
85. Medina-Ramírez, I.E.; Díaz de León-Macias, C.E.; Pedroza-Herrera, G.; Gonzáles-Segovia, R.; Zapien, J.A.; Rodríguez-López, J.L. Evaluation of the Biocompatibility and Growth Inhibition of Bacterial Biofilms by ZnO, Fe_3O_4 and ZnO@Fe_3O_4 Photocatalytic Magnetic Materials. *Ceram. Int.* **2020**, *46*, 8979–8994. [CrossRef]
86. Liu, H.; Wu, J.; Min, J.H.; Zhang, X.; Kim, Y.K. Tunable Synthesis and Multifunctionalities of Fe_3O_4-ZnO Hybrid Core-Shell Nanocrystals. *Mater. Res. Bull.* **2013**, *48*, 551–558. [CrossRef]
87. Madhubala, V.; Kalaivani, T. Phyto and Hydrothermal Synthesis of Fe_3O_4@ZnO Core-Shell Nanoparticles Using Azadirachta Indica and Its Cytotoxicity Studies. *Appl. Surf. Sci.* **2018**, *449*, 584–590. [CrossRef]
88. Manikandan, A.; Yogasundari, M.; Thanrasu, K.; Dinesh, A.; Raja, K.K.; Slimani, Y.; Jaganathan, S.K.; Srinivasan, R.; Baykal, A. Structural, Morphological and Optical Properties of Multifunctional Magnetic-Luminescent ZnO@Fe_3O_4 Nanocomposite. *Phys. E Low Dimens. Syst. Nanostruct.* **2020**, *124*, 114291. [CrossRef]
89. Ahadpour Shal, A.; Jafari, A. Study of Structural and Magnetic Properties of Superparamagnetic Fe_3O_4-ZnO Core-Shell Nanoparticles. *J. Supercond. Nov. Magn.* **2014**, *27*, 1531–1538. [CrossRef]
90. Aljohar, A.Y.; Muteeb, G.; Zia, Q.; Siddiqui, S.; Aatif, M.; Farhan, M.; Khan, M.F.; Alsultan, A.; Jamal, A.; Alshoaibi, A.; et al. Anticancer Effect of Zinc Oxide Nanoparticles Prepared by Varying Entry Time of Ion Carriers against A431 Skin Cancer Cells In Vitro. *Front. Chem.* **2022**, *10*, 1069450. [CrossRef]
91. Gudkov, S.V.; Burmistrov, D.E.; Serov, D.A.; Rebezov, M.B.; Semenova, A.A.; Lisitsyn, A.B. A Mini Review of Antibacterial Properties of ZnO Nanoparticles. *Front. Phys.* **2021**, *9*, 641481. [CrossRef]
92. Wang, J.; Yang, J.; Li, X.; Wang, D.; Wei, B.; Song, H.; Li, X.; Fu, S. Preparation and Photocatalytic Properties of Magnetically Reusable Fe_3O_4@ZnO Core/Shell Nanoparticles. *Phys. E Low Dimens. Syst. Nanostruct.* **2016**, *75*, 66–71. [CrossRef]
93. Sin, J.C.; Tan, S.Q.; Quek, J.A.; Lam, S.M.; Mohamed, A.R. Facile Fabrication of Hierarchical Porous ZnO/Fe_3O_4 Composites with Enhanced Magnetic, Photocatalytic and Antibacterial Properties. *Mater. Lett.* **2018**, *228*, 207–211. [CrossRef]
94. Tang, S.; Lan, Q.; Liang, J.; Chen, S.; Liu, C.; Zhao, J.; Cheng, Q.; Cao, Y.C.; Liu, J. Facile Synthesis of Fe_3O_4@PPy Core-Shell Magnetic Nanoparticles and Their Enhanced Dispersity and Acid Stability. *Mater. Des.* **2017**, *121*, 47–50. [CrossRef]
95. Mohammadi, M.A.; Asghari, S.; Aslibeiki, B. Surface Modified Fe_3O_4 Nanoparticles: A Cross-Linked Polyethylene Glycol Coating Using Plasma Treatment. *Surf. Interfaces* **2021**, *25*, 101271. [CrossRef]
96. Munir, T.; Mahmood, A.; Rasul, A.; Imran, M.; Fakhar-e-Alam, M. Biocompatible Polymer Functionalized Magnetic Nanoparticles for Antimicrobial and Anticancer Activities. *Mater. Chem. Phys.* **2023**, *301*, 127677. [CrossRef]
97. Bekaroğlu, M.G.; Alemdar, A.; İşçi, S. Comparison of Ionic Polymers in the Targeted Drug Delivery Applications as the Coating Materials on the Fe_3O_4 Nanoparticles. *Mater. Sci. Eng. C* **2019**, *103*, 109838. [CrossRef]
98. Thi, T.T.H.; Tran, D.H.N.; Bach, L.G.; Quang, H.V.; Nguyen, D.C.; Park, K.D.; Nguyen, D.H. Functional Magnetic Core-Shell System-Based Iron Oxide Nanoparticle Coated with Biocompatible Copolymer for Anticancer Drug Delivery. *Pharmaceutics* **2019**, *11*, 120. [CrossRef]
99. Ding, Y.; Shen, S.Z.; Sun, H.; Sun, K.; Liu, F.; Qi, Y.; Yan, J. Design and Construction of Polymerized-Chitosan Coated Fe_3O_4 Magnetic Nanoparticles and Its Application for Hydrophobic Drug Delivery. *Mater. Sci. Eng. C* **2015**, *48*, 487–498. [CrossRef]
100. Yeamsuksawat, T.; Zhao, H.; Liang, J. Characterization and Antimicrobial Performance of Magnetic Fe_3O_4@Chitosan@Ag Nanoparticles Synthesized via Suspension Technique. *Mater. Today Commun.* **2021**, *28*, 102481. [CrossRef]